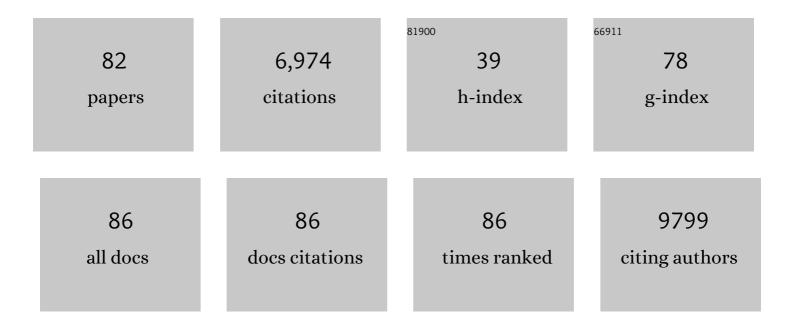
List of Publications by Year in descending order

Source: https://exaly.com/author-pdf/2794768/publications.pdf Version: 2024-02-01



#	Article	IF	CITATIONS
1	Suppressing photoinduced charge recombination at the BiVO4 NiOOH junction by sandwiching an oxygen vacancy layer for efficient photoelectrochemical water oxidation. Journal of Colloid and Interface Science, 2022, 608, 1116-1125.	9.4	19
2	Surface Molecular Functionalization of Unusual Phase Metal Nanomaterials for Highly Efficient Electrochemical Carbon Dioxide Reduction under Industryâ€Relevant Current Density. Small, 2022, 18, e2106766.	10.0	30
3	Non-centrosymmetric Hollow BiOCl Nanocaps with Tailored Openings for the Photocatalytic Degradation of Rhodamine B. ACS Applied Nano Materials, 2022, 5, 2326-2334.	5.0	11
4	Designer Goldâ€Framed Palladium Nanocubes for Plasmonâ€Enhanced Electrocatalytic Oxidation of Ethanol. Chemistry - A European Journal, 2022, 28, .	3.3	5
5	Synthesis of Chiral Au Nanocrystals with Precise Homochiral Facets for Enantioselective Surface Chemistry. Nano Letters, 2022, 22, 2915-2922.	9.1	42
6	Highly enantioselective electrochemical sensing based on helicoid Au nanoparticles with intrinsic chirality. Sensors and Actuators B: Chemical, 2022, 362, 131757.	7.8	16
7	Lead-free hybrid perovskite photocatalysts: surface engineering, charge-carrier behaviors, and solar-driven applications. Journal of Materials Chemistry A, 2022, 10, 12296-12316.	10.3	29
8	Surface engineering of Rh-modified Pd nanocrystals by colloidal underpotential deposition for electrocatalytic methanol oxidation. Nanoscale, 2021, 13, 5284-5291.	5.6	13
9	Boosting chiral amplification in plasmon-coupled circular dichroism using discrete silver nanorods as amplifiers. Chemical Communications, 2021, 57, 7390-7393.	4.1	6
10	Selective Epitaxial Growth of Rh Nanorods on 2H/ <i>fcc</i> Heterophase Au Nanosheets to Form 1D/2D Rh–Au Heterostructures for Highly Efficient Hydrogen Evolution. Journal of the American Chemical Society, 2021, 143, 4387-4396.	13.7	56
11	Unconventional-Phase Crystalline Materials Constructed from Multiscale Building Blocks. Chemical Reviews, 2021, 121, 5830-5888.	47.7	57
12	A trace ppb-level electrochemical H2S sensor based on ultrathin Pt nanotubes. Talanta, 2021, 233, 122539.	5.5	19
13	Unveiling the Actual Catalytic Sites in Nanozymeâ€Catalyzed Oxidation of <i>o</i> â€Phenylenediamine. Small, 2021, 17, e2104083.	10.0	21
14	Facet-Dependent Catalytic Performance of Au Nanocrystals for Electrochemical Nitrogen Reduction. ACS Applied Materials & Interfaces, 2020, 12, 41613-41619.	8.0	42
15	Dual roles of underpotential deposition in the synthesis of tetrahexahedral Pd–Ag alloy nanocrystals. Chemical Communications, 2020, 56, 14849-14852.	4.1	7
16	Unveiling One-Pot Template-Free Fabrication of Exquisite Multidimensional PtNi Multicube Nanoarchitectonics for the Efficient Electrochemical Oxidation of Ethanol and Methanol with a Great Tolerance for CO. ACS Applied Materials & Interfaces, 2020, 12, 31309-31318.	8.0	73
17	Ethylene Selectivity in Electrocatalytic CO ₂ Reduction on Cu Nanomaterials: A Crystal Phase-Dependent Study. Journal of the American Chemical Society, 2020, 142, 12760-12766.	13.7	183
18	<i>In-Situ</i> Probing of Crystal-Phase-Dependent Photocatalytic Activities of Au Nanostructures by Surface-Enhanced Raman Spectroscopy. , 2020, 2, 409-414.		22

#	Article	IF	CITATIONS
19	Heterophase fcc-2H-fcc gold nanorods. Nature Communications, 2020, 11, 3293.	12.8	92
20	Unusual 4H-phase twinned noble metal nanokites. Nature Communications, 2019, 10, 2881.	12.8	25
21	PtCu–O highly excavated octahedral nanostructures built with nanodendrites for superior alcohol electrooxidation. Journal of Materials Chemistry A, 2019, 7, 8568-8572.	10.3	32
22	Highly Excavated Octahedral Nanostructures Integrated from Ultrathin Mesoporous PtCu ₃ Nanosheets: Construction of Threeâ€Dimensional Open Surfaces for Enhanced Electrocatalysis. Small, 2019, 15, e1804407.	10.0	19
23	Modulating the oxophilic properties of inorganic nanomaterials for electrocatalysis of small carbonaceous molecules. Nano Today, 2019, 29, 100802.	11.9	20
24	Atomic origins of high electrochemical CO ₂ reduction efficiency on nanoporous gold. Nanoscale, 2018, 10, 8372-8376.	5.6	46
25	Hierarchical concave layered triangular PtCu alloy nanostructures: rational integration of dendritic nanostructures for efficient formic acid electrooxidation. Nanoscale, 2018, 10, 9369-9375.	5.6	28
26	Tip-Selective Growth of Silver on Gold Nanostars for Surface-Enhanced Raman Scattering. ACS Applied Materials & Interfaces, 2018, 10, 14850-14856.	8.0	46
27	Crystal phase-based epitaxial growth of hybrid noble metal nanostructures on 4H/fcc Au nanowires. Nature Chemistry, 2018, 10, 456-461.	13.6	220
28	Pressure-Induced Phase Engineering of Gold Nanostructures. Journal of the American Chemical Society, 2018, 140, 15783-15790.	13.7	68
29	Two-Dimensional Metal Nanomaterials: Synthesis, Properties, and Applications. Chemical Reviews, 2018, 118, 6409-6455.	47.7	711
30	A Novel Photochemical Method for the Synthesis of Au Triangular Nanoplates inside Nanocavity of Mesoporous Silica Shells. Journal of Physical Chemistry C, 2017, 121, 9572-9578.	3.1	18
31	Shaping Gold Nanocrystals in Dimethyl Sulfoxide: Toward Trapezohedral and Bipyramidal Nanocrystals Enclosed by {311} Facets. Journal of the American Chemical Society, 2017, 139, 5817-5826.	13.7	48
32	Ultrathin Twoâ€Ðimensional Organic–Inorganic Hybrid Perovskite Nanosheets with Bright, Tunable Photoluminescence and High Stability. Angewandte Chemie - International Edition, 2017, 56, 4252-4255.	13.8	206
33	A Generalized Method for the Synthesis of Ligand-Free M@SiO ₂ (M = Ag, Au, Pd, Pt) Yolk–Shell Nanoparticles. Langmuir, 2017, 33, 3281-3286.	3.5	22
34	lodide-Switched Deposition for the Synthesis of Segmented Pd–Au–Pd Nanorods: Crystal Facet Matters. Langmuir, 2017, 33, 12254-12259.	3.5	5
35	New electrochemiluminescence catalyst: Cu2O semiconductor crystal and the enhanced activity of octahedra synthesized by iodide ions coordination. Materials Research Express, 2017, 4, 115021.	1.6	3
36	Submonolayered Ru Deposited on Ultrathin Pd Nanosheets used for Enhanced Catalytic Applications. Advanced Materials, 2016, 28, 10282-10286.	21.0	148

#	Article	IF	CITATIONS
37	Concave and duck web-like platinum nanopentagons with enhanced electrocatalytic properties for formic acid oxidation. Journal of Materials Chemistry A, 2016, 4, 807-812.	10.3	27
38	Pd–Pb Alloy Nanocrystals with Tailored Composition for Semihydrogenation: Taking Advantage of Catalyst Poisoning. Angewandte Chemie, 2015, 127, 8389-8392.	2.0	27
39	Pd–Pb Alloy Nanocrystals with Tailored Composition for Semihydrogenation: Taking Advantage of Catalyst Poisoning. Angewandte Chemie - International Edition, 2015, 54, 8271-8274.	13.8	125
40	A Platinum Highly Concave Cube with one Leg on each Vertex as an Advanced Nanocatalyst for Electrocatalytic Applications. ChemCatChem, 2015, 7, 1064-1069.	3.7	24
41	Tuning Interior Nanogaps of Double-shelled Au/Ag Nanoboxes for Surface-Enhanced Raman Scattering. Scientific Reports, 2015, 5, 8382.	3.3	35
42	A Platinum Highly Concave Cube with one Leg on each Vertex as an Advanced Nanocatalyst for Electrocatalytic Applications. ChemCatChem, 2015, 7, 1033-1033.	3.7	0
43	Solvothermal synthesis of metal nanocrystals and their applications. Nano Today, 2015, 10, 240-267.	11.9	206
44	Highly Symmetric Gold Nanostars: Crystallographic Control and Surface-Enhanced Raman Scattering Property. Journal of the American Chemical Society, 2015, 137, 10460-10463.	13.7	261
45	Sandwich-structured Fe ₂ O ₃ @SiO ₂ @Au nanoparticles with magnetoplasmonic responses. Journal of Materials Chemistry C, 2015, 3, 11645-11652.	5.5	13
46	Metallic Nanostructures: Fundamentals. , 2015, , 1-47.		2
47	Controlled Synthesis of Palladium Concave Nanocubes with Sub-10-Nanometer Edges and Corners for Tunable Plasmonic Property. Chemistry of Materials, 2014, 26, 2180-2186.	6.7	72
48	Volume-confined synthesis of ligand-free gold nanoparticles with tailored sizes for enhanced catalytic activity. Chemical Physics Letters, 2014, 613, 95-99.	2.6	15
49	Dodecahedral Gold Nanocrystals: The Missing Platonic Shape. Journal of the American Chemical Society, 2014, 136, 3010-3012.	13.7	39
50	Surface Plasmon-Driven Water Reduction: Gold Nanoparticle Size Matters. Journal of the American Chemical Society, 2014, 136, 9842-9845.	13.7	301
51	One-pot synthesis of gold nanorods using binary surfactant systems with improved monodispersity, dimensional tunability and plasmon resonance scattering properties. Nanotechnology, 2014, 25, 125601.	2.6	23
52	Synthesis of Convex Hexoctahedral Palladium@Gold Core–Shell Nanocrystals with {431} High-Index Facets with Remarkable Electrochemiluminescence Activities. ACS Nano, 2014, 8, 5953-5958.	14.6	76
53	Pd@Au core–shell nanocrystals with concave cubic shapes: kinetically controlled synthesis and electrocatalytic properties. Faraday Discussions, 2013, 164, 175.	3.2	18
54	Synthesis and electrocatalytic properties of tetrahexahedral, polyhedral, and branched Pd@Au core–shell nanocrystals. Chemical Communications, 2013, 49, 8836.	4.1	23

#	Article	IF	CITATIONS
55	A Template-Free and Surfactant-Free Method for High-Yield Synthesis of Highly Monodisperse 3-Aminophenol–Formaldehyde Resin and Carbon Nano/Microspheres. Macromolecules, 2013, 46, 140-145.	4.8	155
56	Facet-dependent electrocatalytic activities of Pd nanocrystals toward the electro-oxidation of hydrazine. Electrochemistry Communications, 2013, 37, 57-60.	4.7	26
57	Seed-mediated growth of noble metal nanocrystals: crystal growth and shape control. Nanoscale, 2013, 5, 3172.	5.6	173
58	Halide Anions as Shape-Directing Agents for Obtaining High-Quality Anisotropic Gold Nanostructures. Chemistry of Materials, 2013, 25, 1392-1399.	6.7	181
59	Synthesis and applications of noble metal nanocrystals with high-energy facets. Nano Today, 2012, 7, 586-605.	11.9	224
60	Seed-mediated growth method for high-quality noble metal nanocrystals. Science China Chemistry, 2012, 55, 2311-2317.	8.2	26
61	Facile synthesis and electrochemiluminescence application of concave trisoctahedral Pd@Au core–shell nanocrystals bound by {331} high-index facets. Chemical Communications, 2011, 47, 10353.	4.1	54
62	Seed-mediated growth of palladium nanocrystals: The effect of pseudo-halide thiocyanate ions. Nanoscale, 2011, 3, 678-682.	5.6	37
63	Crystallographic control of noble metal nanocrystals. Nano Today, 2011, 6, 265-285.	11.9	175
64	Shape-Controlled Synthesis of Single-Crystalline Palladium Nanocrystals. ACS Nano, 2010, 4, 1987-1996.	14.6	380
65	Effect of hydroxyl and amino groups on electrochemiluminescence activity of tertiary amines at low tris(2,2′-bipyridyl)ruthenium(II) concentrations. Talanta, 2010, 81, 44-47.	5.5	40
66	Determination of isocyanates by capillary electrophoresis with tris(2,2′â€bipyridine)ruthenium(II) electrochemiluminescence. Electrophoresis, 2009, 30, 3926-3931.	2.4	20
67	Hydrogen peroxide biosensor based on direct electrochemistry of soybean peroxidase immobilized on single-walled carbon nanohorn modified electrode. Biosensors and Bioelectronics, 2009, 24, 1159-1163.	10.1	64
68	Simultaneous electrochemical determination of uric acid, dopamine, and ascorbic acid at single-walled carbon nanohorn modified glassy carbon electrode. Biosensors and Bioelectronics, 2009, 25, 940-943.	10.1	214
69	Selective Synthesis of Single-Crystalline Rhombic Dodecahedral, Octahedral, and Cubic Gold Nanocrystals. Journal of the American Chemical Society, 2009, 131, 697-703.	13.7	316
70	Electrochemiluminescence from tris(2,2′-bipyridyl)ruthenium(II)–graphene–Nafion modified electrode. Talanta, 2009, 79, 165-170.	5.5	129
71	Single-walled carbon nanohorn as new solid-phase extraction adsorbent for determination of 4-nitrophenol in water sample. Talanta, 2009, 79, 1441-1445.	5.5	91
72	CEC with tris(2,2′â€bipyridyl) ruthenium(II) electrochemiluminescent detection. Electrophoresis, 2008, 29, 4475-4481.	2.4	13

#	Article	IF	CITATIONS
73	Carbon-supported Pd nanocatalyst modified by non-metal phosphorus for the oxygen reduction reaction. Journal of Power Sources, 2008, 182, 91-94.	7.8	46
74	Amperometric glucose biosensor based on single-walled carbon nanohorns. Biosensors and Bioelectronics, 2008, 23, 1887-1890.	10.1	188
75	Glucose biosensor based on gold nanoparticle-catalyzed luminol electrochemiluminescence on a three-dimensional sol–gel network. Electrochemistry Communications, 2008, 10, 1250-1253.	4.7	97
76	Seed-Mediated Growth of Nearly Monodisperse Palladium Nanocubes with Controllable Sizes. Crystal Growth and Design, 2008, 8, 4440-4444.	3.0	230
77	Environmentally Friendly and Highly Sensitive Ruthenium(II) Tris(2,2′-bipyridyl) Electrochemiluminescent System Using 2-(Dibutylamino)ethanol as Co-Reactant. Angewandte Chemie - International Edition, 2007, 46, 421-424.	13.8	288
78	Rotating minidisk–disk electrodes. Electrochemistry Communications, 2007, 9, 1434-1438.	4.7	10
79	Tris(2,2′-bipyridyl)ruthenium(II) electrochemiluminescent detection of coreactants containing aromatic diol group by the interaction between diol and borate anion. Electrochemistry Communications, 2007, 9, 2666-2670.	4.7	18
80	Application of Ceramic Carbon Materials for Solid-Phase Extraction of Organic Compounds. Analytical Chemistry, 2006, 78, 1345-1348.	6.5	24
81	Copper and iron mediated growth of surfactantâ€free PtCu and PtFe advanced electrocatalysts for water oxidation and oxygen reduction. Electrochemical Science Advances, 0, , e2100033.	2.8	1
82	Hard nanocrystalline gold materials prepared via high-pressure phase transformation. Nano Research, 0, , .	10.4	3